Atmos. Chem. Phys. Discuss., 14, 30727–30759, 2014
www.atmos-chem-phys-discuss.net/14/30727/2014/
doi:10.5194/acpd-14-30727-2014

Atmospheric Chemistry and Physics Discussions

Sources of black carbon aerosols in South Asia and surrounding regions during the Integrated Campaign for Aerosols, Gases and Radiation Budget (ICARB)

R. Kumar[1,2], M. C. Barth[2], V. S. Nair[3], G. G. Pfister[2], S. S. Babu[3], S. K. Satheesh[4], K. K. Moorthy[5], and G. R. Carmichael[6]

[1]Advanced Study Program, National Center for Atmospheric Research, Boulder, USA
[2]Atmospheric Chemistry Division, National Center for Atmospheric Research, Boulder, USA
[3]Space Physical Laboratory, Vikram Sarabhai Space Center, Thiruvanantpuram, India
[4]Centre for Atmospheric and Oceanic Sciences, Indian Institute of Science, Bangalore, India
[5]Indian Space Research Organization (Hq), New BEL Road, Bangalore, India
[6]Center for Global and Regional Environmental Research, University of Iowa, Iowa City, IA 52242, USA

Received: 24 August 2014 – Accepted: 6 November 2014 – Published: 5 December 2014

Correspondence to: R. Kumar (rkumar@ucar.edu)

Published by Copernicus Publications on behalf of the European Geosciences Union.

ACPD
14, 30727–30759, 2014

Abstract

The dominant sources of black carbon (BC) in South Asia and surrounding regions are inferred during March–May 2006 (Integrated Campaign for Aerosols, Gases and Radiation Budget, ICARB) period by introducing BC tracers in the Weather Research and Forecasting Model coupled with Chemistry. The model reproduced the magnitude, temporal and spatial variability of BC distribution observed during the ICARB ship-cruise. Average and SD (representing the spatial and temporal variability) in observed and modeled BC mass concentrations along the ship-track are estimated as 755 ± 734 and $732 \pm 913\,\mathrm{ng\,m^{-3}}$ respectively. Average modeled values at most of the inland stations were also found to fall within the range of observed values. Model results show that ICARB measurements were fairly well representative of the Arabian Sea and the Bay of Bengal during the pre-monsoon season. Results show that anthropogenic and biomass burning emissions, respectively, accounted for 70 and 28 % of the average $\pm$ SD BC mass concentration ($1480 \pm 5920\,\mathrm{ng\,m^{-3}}$) in South Asia. BC emissions from residential (49 %) and industrial (37 %) sectors appear to be the major anthropogenic sources, except in the Himalayas where vehicular emissions dominated. We find that, while all parts of continental India contributed to anthropogenic BC over the Bay of Bengal, contribution over the Arabian Sea came mostly from southern Peninsula. We also show that regional-scale transport of anthropogenic emissions contribute up to 30 % of BC mass concentrations in western and eastern India, suggesting that it is important to consider non-local sources along with the local emissions while designing strategies for mitigating BC emissions.

1 Introduction

Black carbon (BC), a byproduct of incomplete combustion, is a key atmospheric aerosol species because it contributes largely to the climate forcing (e.g. Ramanathan and Carmichael, 2008) and, along with other fine particulates, adversely affects human

ACPD
14, 30727–30759, 2014

health (e.g. Dockery and Stone, 2007). BC is emitted from various sources including industries, motor vehicles, power plants, residential solid biofuel burning, and open biomass burning of forests, savannas and crop residues. The total global emissions of BC aerosol estimated using bottom-up approaches are 7500 Gg year^{-1} in the year 2000 with an uncertainty range of 2000 to 29 000 (Bond et al., 2013). BC has very low chemical reactivity in the atmosphere and is removed primarily by wet or dry deposition at the surface with wet deposition representing 70–85 % of the total loss (Pöschl, 2005). The average atmospheric lifetime of BC is estimated to be about a week (Bond et al., 2013) enabling BC aerosols to undergo regional and intercontinental transport.

Different emission sources of BC show strong regional variation (Lawrence and Lelieveld, 2010; Bond et al., 2013) and South Asia with its large population density involved in a wide range of human activities is considered to be one of the hotspots of BC emission (Bond et al., 2007). In addition, different emission inventories show an increasing trend in BC emissions over South Asia (Granier et al., 2011). Large emissions of BC in South Asia lead to BC-induced radiative perturbation which is significantly higher than the globally averaged estimates (Babu et al., 2004; Ramanathan and Carmichael, 2008). Model estimates show that this forcing has the potential to affect the Asian Summer Monsoon through different mechanisms (Ramanathan et al., 2005; Lau et al., 2006), such as heating of the elevated Himalayas (e.g. Menon et al., 2010) and melting of glaciers (e.g. Yasunari et al., 2010).

Many efforts have been made to measure BC mass concentration, document its diurnal, seasonal and spectral (absorption) characteristics and estimate local scale BC-induced radiative perturbation in a wide range of atmospheric conditions (urban, rural, marine and high altitude mountains) in South Asia (e.g. Satheesh and Ramanathan, 2000; Babu et al., 2004; Beegum et al., 2009; Gustafsson et al., 2009; Nair et al., 2008, 2013; Marrapu et al., 2014). The regional and global scale radiative impacts of BC and other short-lived pollutants emitted from different sectors have also been estimated in some global modeling studies (e.g. Reddy et al., 2005; Unger et al., 2009, 2010; Verma et al., 2011). However, the relative contributions of different emission sources

ACPD
14, 30727–30759, 2014

to atmospheric BC mass concentrations are still unknown for South Asia except for the Delhi region, where the majority of the atmospheric BC is attributed to emissions from transportation (~ 59 %) and domestic (~ 32 %) sectors (Marrapu et al., 2014).

In light of the above conditions, the main objective of this study is to determine the most important sources of BC aerosols in the atmosphere of South Asia and surrounding regions. To address this objective, we introduce source, sector and region specific BC tracers in the Weather Research and Forecasting Model coupled (Skamarock et al., 2008) with Chemistry (WRF-Chem) (Grell et al., 2005; Fast et al., 2006). This study focuses on the period of March–May 2006 because of the availability of BC measurements made as a part of the Integrated Campaign for Aerosols, Gases and Radiation Budget (ICARB) (Moorthy et al., 2008). ICARB was an integrated multi-instrument, multi-platform field campaign and provided extensive co-located measurements of several aerosol parameters and trace gases over the Bay of Bengal, northern Indian Ocean and the Arabian Sea. ICARB observations revealed large spatio-temporal heterogeneities in several aerosol parameters including the BC mass concentrations and trace gases over the oceanic regions around India. A major finding was observations of significantly higher pollution loadings in the BoB as compared to the AS (Moorthy et al., 2008; Nair et al., 2008; Srivastava et al., 2012). In this study, we will also use WRF-Chem simulations to understand the reasons behind these observed spatio-temporal heterogeneities in the distribution of BC.

We begin with a description of ICARB observations, WRF-Chem configuration and implementation of BC tracers in the WRF-Chem. In the Results section, we first evaluate the model performance and then quantify the contribution of different emission sources and sectors to total BC loading and demonstrate the importance of regional transport in distribution of BC in the atmosphere of South Asia.

ACPD
14, 30727–30759, 2014

2 Experimental design

We use version 3.5.1 of the WRF-Chem model to simulate the distribution of BC in South Asia and surrounding regions. Recently, we set-up WRF-Chem over South Asia and demonstrated that WRF-Chem is able to capture observed variations in meteorology (Kumar et al., 2012a), gas-phase chemistry (Kumar et al., 2012b, 2013) and dust aerosols (Kumar et al., 2014a, 2014b) over South Asia. However, the model's ability to simulate BC in South Asia and surrounding regions has not been tested so far. In this study, we attempt to fill this gap by comparing WRF-Chem simulated BC with extensive measurements of BC made over the Bay of Bengal (BoB) and the Arabian Sea (AS) during 18 March–11 May 2006 as a part of the ocean segment of the ICARB (see Fig. 1 for ship-track) (Moorthy et al., 2008), and average BC values reported at 12 inland stations in the model domain.

During the ocean segment of ICARB, a special laboratory was configured at the top deck of the ship called "Sagar Kanya" and ambient air was drawn from a height of about 10 m a.s.l. into various instruments deployed for measurements of trace gases and aerosols. BC mass concentrations were measured using an aethalometer (AE 21 of Magee Scientific) operated at a time base of 5 min and flow rate of 5 L min^{-1}. Further details of the ship-cruise track, measurement set-up, uncertainties, quality control and analysis of BC measurements, and meteorological conditions during ICARB are discussed in Nair et al. (2008). In addition, we use average BC values reported for March to May at 12 stations in the model domain (Table 1). These stations are located in a wide range of chemical environments with Delhi, Kanpur, Kharagpur and Dibrugarh representing urban/semi-urban sites, Lhasa representing a high altitude urban site, Trivandrum representing a coastal semi-urban site, Nainital, Nagarkot, Langtang and Nepal Climate Observatory – Pyramid (NCO-P) representing high altitude cleaner sites, and Minicoy and Port-Blair representing island sites, respectively.

The WRF-Chem domain covers South Asia and surrounding oceanic regions with a horizontal grid spacing of 36 km (Fig. 1) and 35 levels from surface to 10 hPa. Aerosol

ACPD
14, 30727–30759, 2014

processes are represented by the Model for Simulating Aerosol Interactions and Chemistry (MOSAIC, Zaveri et al., 2008) using 4 size bins. MOSAIC treats black carbon as internally mixed with other major aerosol species including sulfate, nitrate, organic carbon, liquid water, methanesulfonate, chloride, carbonate, ammonium, sodium, calcium, and other inorganics (including dust) within each size bin. The aerosol particles are considered as hydrophilic and can activate to form cloud droplets. Aerosol particles are subjected to both dry and wet deposition (in- and below-cloud scavenging) where the dry deposition module follows Binkowski and Shankar (1995) and wet deposition module follows Easter et al. (2004). Wet deposition represents the major loss (~ 84 %) process for BC in our model domain. The gas-phase chemistry is represented by Model for Ozone and Related Tracers (MOZART) chemical mechanism (Emmons et al., 2010; Knote et al., 2014). Initial and lateral boundary conditions for meteorological and chemical fields are obtained from 6 hourly NCEP Final Analysis Fields and MOZART-4 results (Emmons et al., 2010) respectively. Analysis nudging is applied to horizontal winds, moisture and temperature above the planetary boundary layer with a nudging coefficient of $3 \times 10^{-4}\,s^{-1}$.

Anthropogenic emissions of BC and other trace species in India and regions due east of India are taken from the Southeast Asia Composition, Clouds and Climate Coupling by Regional Study (SEAC^{4}RS) emissions inventory (Lu and Streets, 2012), while those in the regions due west of India and the shipping emissions are taken from MACCity emission inventory (Granier et al., 2011). The spatial distribution of anthropogenic BC emissions is shown in Fig. 1 and shows highest values over the Indo–Gangetic Plain. The total annual anthropogenic BC emissions in this combined (SEAC^{4}RS+MACCity) emission inventory for South Asia (60–100° E, 5–37° N) are estimated as ~ 1195 Gg year^{-1}, which are comparable to other regional inventories such as System for Air quality Forecasting And Research-India (SAFAR-India: ~ 1110 Gg year^{-1}) and Regional Emission Inventory for Asia (REAS: ~ 1170 Gg year^{-1}) but are significantly higher compared to Intercontinental chemical Transport Experiment Phase B inventory (INTEX-B: ~ 550 Gg year^{-1}). Note that SAFAR-India does

ACPD
14, 30727–30759, 2014

not provide emissions outside India. Biomass burning emissions of trace gases and aerosols are obtained from the Fire Inventory from NCAR (Wiedinmyer et al., 2011) and are distributed in the model vertically following the online plume-rise module (Freitas et al., 2007). For the nearly two-month ICARB period (18 March–11 May 2006), total South Asian biomass burning emissions (356 Gg) of BC are higher than the total anthropogenic emissions (229 Gg) but ∼ 80 % of the biomass burning activity occurs in Burma (93–100° E, 15–30° N). Note that biomass burning represents emissions only from open fires, while emissions from residential soild bio-fuel burning are included in the anthropogenic emissions. The parameterization used for other atmospheric processes along with schemes used for the biogenic and dust emissions are listed in Table 2.

This study implements 13 BC tracers in the WRF-Chem model to track BC emitted from different source types, sectors and regions. The tracer approach has been used previously in WRF-Chem to study the budget of CO in the USA (Pfister et al., 2011; Boynard et al., 2012) and South Asia (Kumar et al., 2013), but BC tracers are implemented for the first time in the model. BC tracers are artificial species added to the simulation and experience the same transport, physical, chemical and loss processes as a standard BC particle. However, the tracers do not affect the standard model results by modifying the radiation, atmospheric processes and aerosol properties.

We account for all sources of BC in the model by tracking BC emitted from anthropogenic (BC-ANT) and biomass burning (BC-BB) sources within the domain, and BC inflow from the lateral domain boundaries (BC-BDY). The BC-BDY tracer includes the contribution from all BC emission sources located outside the selected domain and therefore its distribution will provide information about background BC levels for South Asia. In addition, we track BC emitted from residential (BC-RES), transport (BC-TRA), industrial (BC-IND) and power-plants (BC-POW) sectors to estimate the contribution of different sectors to anthropogenic BC loadings. BC emissions from industrial, power and transportation sectors are mostly due to combustion of fossil fuels, while those from residential sectors are mostly due to biofuel combustion.

ACPD
14, 30727–30759, 2014

Five regional tracers track BC emitted from North, West, East and South India, and Burma (Fig. 1). Anthropogenic emissions of BC from outside these five regions are also tracked separately and are classified as other regions. The initial and boundary conditions for all BC tracers are set to zero because MOZART-4 does not include such a tracer classification except boundary conditions for BC-BDY, which are set equal to BC from MOZART-4. The model simulations started on 15 February 2006 at 00:00 UTC with a time step of 180 s, and model results are output every hour. The tracers are assumed to be well spun-up when the sum of BC tracers (BC_{trac} = BC-ANT + BC-BB + BC-BDY) approaches the total simulated BC. The time series of the relative difference between domain-wide averaged BC and BC_{trac} (Fig. 2) at the first, 10th and 20th model level shows that the difference rapidly approaches 0 % in the first 15 days of model run and remains close to zero for the rest of the model simulation. Thus, all tracers are spun up by 20 January 2011.

3 Model evaluation

We first examine the ability of WRF-Chem in reproducing the variability and features of the BC distribution observed over the BoB and the AS during the ICARB campaign (Nair et al., 2008). The WRF-Chem predicted BC mass concentrations (surface layer) are bi-linearly interpolated to the ICARB ship track and compared to hourly ICARB BC measurements (Fig. 3a). Both the model and observations show significantly higher BC levels in the BoB as compared to the AS. The average observed and modeled BC mass concentrations along the ship-track agree well (755 ± 734 ng m^{-3} and 732 ± 913 ng m^{-3} respectively). This agreement is in contrast with previous modeling studies over South Asia which found a large underestimation of BC mass concentration by chemical transport models (e.g. Nair et al., 2012). The differences between this and previous studies could be due to use of both a different emission inventory and a different chemical transport model. However, some differences between WRF-Chem and observations are also discerned here and could be related to the uncertainties in BC emission estimates,

ACPD
14, 30727–30759, 2014

model transport and parameterization of aerosol processes. To evaluate the model's ability in capturing the spatial variability of BC observed along the ICARB ship-track, we compare co-located observed and WRF-Chem predicted latitudinal distribution of BC mass concentrations (Fig. 4). Both the model and observed values are averaged over 1° latitude bins for this comparison. The modeled values generally matches with the observed values within one SD, however, large differences are seen in the northern coastal BoB (19–20° N), where the SD increases, indicating a lot of spatial variability in this region. The model also captures the latitudinal gradients of opposite sense in the BoB and AS with both the model and observations showing an increasing tendency in BC with latitude in the BoB but a decreasing tendency in the AS.

The ICARB observations provide only a snapshot of the BC distribution because the ship was moving continuously in space and time (Fig. 1). Here, we analyze the spatial distribution of BC mass concentrations averaged over the ICARB period (Fig. 5a) to assess the representativeness of the ICARB ship-borne observations. As for the ship observations, the average modeled spatial distribution also shows more elevated BC levels in the BoB than the AS and latitudinal gradient of opposite sense in the BoB and the AS. This consistency of features deduced from ICARB observations with average model results indicates that ICARB ship-cruise was fairly well representative of the BoB and the AS during the pre-monsoon season.

In addition, we assess the model performance over the land by comparing WRF-Chem predicted BC values with average observed values reported for March to May at 12 stations in the model domain (Table 1). Average observed and modeled values at these sites range from 0.065 to 12 $\mu g\,m^{-3}$ and 0.32–7.4 $\mu g\,m^{-3}$, respectively. Average modeled values either fall within or are close to the observed range at most of the sites but show larger differences ($> 2\,\mu g\,m^{-3}$) especially at the urban/semi-urban sites (Delhi, Kharagpur, Diburgarh and Lhasa). This could be partly due to error in the BC emission inventory and partly due to use of coarser model resolution (36 km^2) because model at this resolution is not able to capture subgrid scale variations in the location of emission sources (roadways, power plants, industries, residential burning etc.). Se-

ACPD
14, 30727–30759, 2014

ungkyu et al. (personal communication) showed that differences between the modeled and observed BC mass concentration in Kathmandu valley can be reduced by a factor of about 4 if the emission sources are appropriately distributed according to their location as compared to the emissions averaged over grids of 5 km^2. Marrapu et al. (2014) also found observed and modeled BC mass concentrations matching within one SD at Delhi using a very high resolution (1.67 km^2) emission inventory.

The results presented above demonstrate the model's ability to simulate the BC distribution in this region. Even though there are differences in urban locations but better agreement between the model and observations along the ICARB ship-track and high altitude cleaner sites indicates that total BC emissions in South Asia are likely right and model results can be used to conduct a source contribution analysis of BC.

4 Source contribution analysis

4.1 The ICARB ship-track

We first identify the sources affecting the ICARB ship-track by analyzing the time series of BC source tracers along the ship-track (Fig. 3b). Model results suggest that anthropogenic emissions within the model domain were the main source of BC observed during ICARB. Biomass burning emission sources did not contribute more than 10 % except during 5–8 April 2006, when the contribution of biomass burning exceeded 50 %. The contribution of BC transported from the domain boundaries to the total BC mass concentration was less than 10 % in the BoB but was up to 40 % in the AS. To identify the regions where anthropogenic emission sources affecting the ICARB ship-track were located, we analyze the contribution of anthropogenic sources located in different regions to the total anthropogenic BC loading in the BoB and the AS (Table 3). The average modeled total anthropogenic BC mass concentrations in the BoB and the AS are estimated as $1019 \pm 1012\,ng\,m^{-3}$, and $241 \pm 457\,ng\,m^{-3}$, respectively, where the SDs represent the large spatial variability in each region (as can be seen in

ACPD
14, 30727–30759, 2014

Fig. 5a). These numbers show that BC concentrations from anthropogenic emissions in the BoB are nearly 4 times stronger than those in the AS. The regional source contribution analysis shows that the ICARB ship-track in the BoB was affected by all parts of India with highest contribution from anthropogenic sources located in East (~ 44 %) and South (~ 32 %) parts of India, while that in the AS had maximum influence from South (~ 83 %) parts of India.

4.2 South Asia

To identify the most important sources of BC in South Asia, we analyze the spatial distributions of percentage contributions of anthropogenic (BC-ANT), biomass burning (BC-BB) and boundary inflow (BC-BDY) to total BC loadings in the model domain (Fig. 5b–d). Model results show large spatial variability in average total BC mass concentrations in South Asia with the highest values (> 5000 ng m^{-3}) in the Indo–Gangetic Plain region, Mumbai–Pune region and Burma (93–100° E, 15–30° N). The BC-ANT distribution shows that anthropogenic emissions account for 60–95 % of the total surface BC over India and in the cleaner regions of the Himalayas, the BoB and the AS. Elevated BC levels over Burma are mainly (> 70 %) due to biomass burning as evident from distribution of BC-BB. Biomass burning also contributes 20–50 % of BC loadings in Nepal, eastern India and eastern BoB. The distribution of BC-BDY shows that emission sources located outside the domain contributes less than 5 % to the BC loading over most parts of India, BoB and Burma, but makes a moderate contribution (up to 25 %) in the AS and the Himalayas.

The spatial distributions of BC source tracers also help us to understand why latitudinal gradients of opposite sense were observed in the BoB and AS, and why BC showed an eastward increase due north of 13° N in the BoB (Nair et al., 2008). The latitudinal gradients of the opposite sense were observed in the BoB and the AS because influence of anthropogenic emissions in the BoB decreased southwards while it increased southwards in the AS (Fig. 5b). BC showed an eastward increase due north of 13° N because eastern BoB was affected by both the anthropogenic and biomass

ACPD
14, 30727–30759, 2014

burning sources while western BoB was affected mostly by the anthropogenic sources (Fig. 5b, c).

The average mass concentrations of BC, BC-ANT, BC-BB and BC-BDY in South Asia (60–100° E, 5–37° N) during the ICARB period are given in Table 4. The contributions of BC-ANT, BC-BB and BC-BDY to the average total BC mass concentrations are estimated at about 70 %, 28 % and 1 %, respectively. Large SD of the average values reflect large spatial heterogeneity of BC mass concentrations.

While it is seen that anthropogenic emissions stand out as the major source of BC in the study domain in general, we identify the contribution of different sectors (such as residential (RES), industrial (IND), transportation (TRA), and power generation (POW)) to total anthropogenic BC loading. This information is important for developing mitigation strategies but such an application would require extension of this analysis at least to one complete year because the BC emissions from biomass burning and residential sectors vary seasonally. We did not conduct a full year analysis because of the limited computational resources. The spatial distributions of these contributions, along with that of the total anthropogenic BC mass concentrations (BC-ANT) are shown in Figs. 5e-5h.

Among the different sectors, residential emissions account for more than half of the anthropogenic BC loading in Nepal, Bangladesh, Burma, Sri Lanka, and Central India, while emissions from industrial sector dominate along the southwest and east Indian coastlines. The dominance of residential biofuel burning sources is consistent with conclusions from previous studies in this region (e.g. Gustafsson et al., 2009). The transport and residential sectors contribute almost equally (30–40 %) to the anthropogenic BC mass concentration loading in Pakistan. In the Himalayan regions, the transport sector (vehicular emissions) contributes to 60–90 % of the anthropogenic BC, while in the BoB and the AS industrial (30–70 %) and residential (30–60 %) emissions dominates. BC emissions from shipping are included in the transport sector and thus we see higher contribution of transport sector in the southern parts of both the BoB and the AS as compared to northern parts. The contribution of BC emissions from power

ACPD
14, 30727–30759, 2014

plants is estimated to be less than 1 % (not shown). The average mass concentrations of BC-RES, BC-IND, BC-TRA and BC-POW in South Asia (60–100° E, 5–37° N) during 18 March–11 May 2006 are given in Table 4. The emissions from residential, industrial, transport and power plant sectors contribute about 49, 37, 13 and 1 %, respectively, to average BC-ANT mass concentrations.

4.3 Local vs. regional anthropogenic sources

In this section, we examine the relative importance of local anthropogenic emissions compared to anthropogenic sources from other parts of South Asia (i.e. regional transport). The spatial distributions of BC emitted from anthropogenic sources in North, West, East and South India, Burma and other regions averaged over 18 March–11 May 2006 at the surface are shown in Fig. 6. Anthropogenic sources in Northern India contribute more than 100 ng m^{-3} to anthropogenic BC loadings in western and eastern parts of India, Burma and the BoB, and slightly influence parts of the AS along western Indian coastline. Northern Indian sources also contribute up to 50 ng m^{-3} in the Himalayan–Tibetan plateau region, but this contribution is smaller than that from other regions (50–200 ng m^{-3}). Analysis of diurnal variations of BC emitted from Northern India and vertical wind component over the Tibetan region (81–90° E, 30–35° N) showed that transport of BC from North India to the Tibetan region likely occurs through upslope winds. However, more observations and fine scale modeling studies are required to lend further confidence in this process. BC emitted by anthropogenic sources in western India contributes significantly to eastern and southern parts of India but the influence (> 20 ng m^{-3}) also reaches to the BoB and parts of AS along western Indian coastline. Anthropogenic sources in eastern India significantly affects BC loadings in Burma, Bay of Bengal and South India but the influence does not reach the AS. South Indian anthropogenic sources affect both the BoB and the AS but the influence is higher in the BoB. Anthropogenic sources located in Burma do not make a significant impact in the BoB and the AS, while those located in other regions affect the southern parts of the BoB in the vicinity of Sri Lanka.

ACPD
14, 30727–30759, 2014

The contributions of BC emitted from different regions of South Asia to the total anthropogenic BC loadings in the five defined regions of South Asia, the AS and the BoB are summarized in Table 3. Here, we also quantify the contribution of local and regional sources to the anthropogenic BC loading in the different regions. The amount of BC due to sources located in a given region itself (e.g. BC-NI for Northern India) is defined as a contribution from local sources, and BC coming from sources outside this region (e.g. BC-WI + BC-EI + BC-SI + BC-BR + BC-OT for Northern India) is defined as contribution from the regional sources. The contribution of local sources is marked in bold font in Table 3. Local sources account for about 90 % of the anthropogenic BC loading in North and South India, but regional sources contribute up to 30 % in West and 21 % in East India. Regional sources make a large contribution of 75 % to the anthropogenic BC loading in Burma. However, it should also be noted that total anthropogenic BC loading in Burma is much smaller than the BC loading due to local biomass burning (Fig. 5b, c). For the AS and the BoB, we find results similar to what we found along the ship-track (Sect. 3.2.1), i.e., anthropogenic BC loadings in the AS is mostly controlled by the sources located in southern India while BoB is affected by anthropogenic sources located in all parts of India.

5 Summary

This study implemented source, sector and region specific BC tracers in the WRF-Chem model to assess the relative importance of different BC sources in South Asia during March–May 2006. The model reproduced the magnitude, temporal and spatial variability of BC distribution observed during the ICARB ship-cruise. The average and SD (representing the spatial and temporal variability) in observed and modeled BC mass concentrations along the ship-track are estimated as $755 \pm 734\,\mathrm{ng\,m^{-3}}$ and $732 \pm 913\,\mathrm{ng\,m^{-3}}$ respectively. Average modeled concentrations at most of the inland stations were also found to fall within the range of observed values, but larger differences were

ACPD
14, 30727–30759, 2014

seen at some urban locations indicating the need for high resolution modeling and emission inventories at urban scales.

Analysis of BC tracers shows that the ICARB ship-track in the BoB was affected by anthropogenic sources located in all parts of India with highest contributions from East (43 %) and South (31 %) India. In contrast, the AS was affected mostly by sources in South India. We find that elevated levels of BC in the BoB were due to a much stronger anthropogenic influence (4 times greater) in the BoB than the AS. The features of the BC distribution deduced from ICARB ship observations were found to be consistent with model results averaged over larger spatial area and time period (18 March–11 May 2006) indicating that ICARB measurements were fairly well representative of the BoB and the AS during the pre-monsoon season.

Average modeled BC mass concentration in South Asia is estimated as $1480 \pm 5920\,\mathrm{ng\,m^{-3}}$ where the high SD reflects the large spatial and temporal variability. Analysis of BC source tracers showed that anthropogenic emissions provided 60–95 % of the total BC loading in South Asia except in Burma where biomass burning played a major role during this period. Biomass burning also contributed more than 20 % to the BC in Nepal, eastern India and eastern BoB. BC emissions from residential (49 %) and industrial (37 %) sectors are identified as major anthropogenic sources in South Asia except in the Himalayas where vehicular emissions dominated. We also find that regional transport plays an important role in distributing BC in South Asia and contributes up to 30 % in West India and upto 21 % in East India.

This study illustrates the potential of integrating in situ observations with chemical transport modeling to understand processes controlling the distribution and variability of BC, and infer the most important sources of BC aerosol. These results can potentially form the basis for the development of BC mitigation strategies in South Asia. However, at least a full year of such source contribution simulations must be conducted to account for changes in regional meteorology, and seasonal variability of sources such as open biomass burning and residential soild fuel burning.

ACPD
14, 30727–30759, 2014

Acknowledgements. We thank C. Knote for providing the basic WRF-Chem configuration used in this study. We thank F. Flocke, S. Madronich and C. Knote for their constructive comments on the manuscript. The datasets of initial and boundary conditions for meteorological fields is downloaded from http://rda.ucar.edu/datasets/ds083.2/. The datasets for initial and boundary conditions for chemical fields, biogenic emissions, biomass burning emissions and programs used to process these datasets are downloaded from the website http://www2.acd.ucar.edu/wrf-chem/. The National Center for Atmospheric Research is supported by the National Science Foundation. Authors acknowledge the ICARB project of ISRO-Geosphere Biosphere Program for providing the data collected onboard *Sagar Kanya*. We acknowledge ECCAD science team for providing emissions datasets.

References

Babu, S. S., Moorthy, K. K., and Satheesh, S. K.: Aerosol black carbon over Arabian Sea during inter monsoon and summer monsoon seasons, Geophys. Res. Lett., 31, L06104, doi:10.1029/2003GL018716, 2004.

Beegum, S. N., Moorthy, K. K., Babu, S. S., Satheesh, S. K., Vinoj, V., Badarinath, K. V. S., Safai, P. D., Devara, P. C. S., Singh, S., Vinod, Dumka, U. C., and Pant, P.: Spatial distribution of aerosol black carbon over India during pre-monsoon season, Atmos. Environ., 43, 1071–1078, doi:10.1016/j.atmosenv.2008.11.042, 2009.

Beljaars, A. C. M.: The parameterization of surface fluxes in large-scale models under free convection, Q. J. Roy. Meteor. Soc., 121, 255–270, 1994.

Binkowski, F. S. and Shankar, U.: The regional particulate matter model: 1. Model description and preliminary results, J. Geophys. Res., 100, 26191–26209, doi:10.1029/95JD02093, 1995.

Bonasoni, P., Laj, P., Marinoni, A., Sprenger, M., Angelini, F., Arduini, J., Bonafè, U., Calzolari, F., Colombo, T., Decesari, S., Di Biagio, C., di Sarra, A. G., Evangelisti, F., Duchi, R., Facchini, MC., Fuzzi, S., Gobbi, G. P., Maione, M., Panday, A., Roccato, F., Sellegri, K., Venzac, H., Verza, GP., Villani, P., Vuillermoz, E., and Cristofanelli, P.: Atmospheric Brown Clouds in the Himalayas: first two years of continuous observations at the Nepal Climate Observatory-Pyramid (5079 m), Atmos. Chem. Phys., 10, 7515–7531, doi:10.5194/acp-10-7515-2010, 2010.

ACPD
14, 30727–30759, 2014

Bond, T. C., Bhardwaj, E., Dong, R., Jogani, R., Jung, S., Roden, C., Streets, D. G., and Trautmann, N. M.: Historical emissions of black and organic carbon aerosol from energy related combustion, 1850–2000, Global Biogeochem. Cy., 21, GB2018, doi:10.1029/2006GB002840, 2007.

Bond, T. C., Doherty, S. J., Fahey, D. W., Forster, P. M., Berntsen, T., DeAngelo, B. J., Flanner, M. G., Ghan, S., Kärcher, B., Koch, D., Kinne, S., Kondo, Y., Quinn, P. K., Sarofim, S., Schultz, M., Venkataraman, C., Zhang, H., Zhang, S., Bellouin, N., Guttikunda, S., Hopke, P. K., Jacobson, M. Z., Kaiser, J. W., Klimont, Z., Lohmann, U., Schwarz, J. P., Shindell, D., Storelvmo, T., Warren, S. G., and Zender, S.: Bounding the role of black carbon in the climate system: a scientific assessment, J. Geophys. Res., 118, 1–173, doi:10.1002/jgrd.50171, 2013.

Boynard, A., Pfister, G. G., and Edwards, D. P.: Boundary layer versus free tropospheric CO budget and variability over the United States during summertime, J. Geophys. Res., 117, D04306, doi:10.1029/2011JD016416, 2012.

Carrico, C. M., Bergin, M. H., Shrestha, A. B., Dibb, J. E., Gomes, L., and Harris, J. M.: The importance of carbon and mineral dust to seasonal aerosol properties in the Nepal Himalayas, Atmos. Environ., 37, 2811–2824, doi:10.1016/S1352-2310(03)00197-3, 2003.

Dockery, D. W. and Stone, P. H.: Cardiovascular risks from fine particulate air pollution, New Engl. J. Med., 365, 511–513, 2007.

Easter, R. C., Ghan, S. J., Zhang, Y., Saylor, R. D., Chapman, E. G., Laulainen, N. S., Abdul-Razzak, H., Leung, L. R., Bian, X., and Zaveri, R. A.: MIRAGE: model description and evaluation of aerosols and trace gases, J. Geophys. Res., 109, D20210, doi:10.1029/2004JD004571, 2004.

Emmons, L. K., Walters, S., Hess, P. G., Lamarque, J.-F., Pfister, G. G., Fillmore, D., Granier, C., Guenther, A., Kinnison, D., Laepple, T., Orlando, J., Tie, X., Tyndall, G., Wiedinmyer, C., Baughcum, S. L., and Kloster, S.: Description and evaluation of the Model for Ozone and Related chemical Tracers, version 4 (MOZART-4), Geosci. Model Dev., 3, 43–67, doi:10.5194/gmd-3-43-2010, 2010.

Fast, J. D., Gustafson Jr., W. I., Easter, R. C., Zaveri, R. A., Barnard, J. C., Chapman, E. G., and Grell, G. A.: Evolution of ozone, particulates, and aerosol direct forcing in an urban area using anew fully-coupled meteorology, chemistry, and aerosol model, J. Geophys. Res., 111, D21305, doi:10.1029/2005JD006721, 2006.

ACPD
14, 30727–30759, 2014

Freitas, S. R., Longo, K. M., Chatfield, R., Latham, D., Silva Dias, M. A. F., Andreae, M. O., Prins, E., Santos, J. C., Gielow, R., and Carvalho Jr., J. A.: Including the sub-grid scale plume rise of vegetation fires in low resolution atmospheric transport models, Atmos. Chem. Phys., 7, 3385–3398, doi:10.5194/acp-7-3385-2007, 2007.

Ginoux, P., Chin, M., Tegen, I., Prospero, J. M., Holben, B., Dubovik, O., and Lin, S. J.: Sources and distributions of dust aerosols simulated with the GOCART model, J. Geophys. Res., 106, 20255–20273, 2001.

Granier, C. Bessagnet, B., Bond, T., D'Angiola, A., van der Gon, H. G., Frost, G. J., Heil, A., Kaiser, J. W., Kinne, S., Klimont, Z., Kloster, S., Lamarque, J.-F., Liousse, C., Masui, T., Meleux, F., Mieville, A., Ohara, T., Raut, J.-C., Riahi, K., Schultz, M. G., Smith, S. J., Thompson, A., van Aardenne, J., van der Werf, G. R., and van Vuuren, D. P.: Evolution of anthropogenic and biomass burning emissions of air pollutants at global and regional scales during the 1980–2010 period, Climatic Change, 109, 163–190, doi:10.1007/s10584-011-0154-1, 2011.

Grell, G. and Devenyi, A. D.: A generalized approach to parameterizing convection combining ensemble and data assimilation techniques, Geophys. Res. Lett., 29, 1693, 2002.

Grell, G. A., Peckham, S. E., Schmitz, R., McKeen, S. A., Frost, G., Skamarock, W. C., and Eder, B.: Fully coupled "online" chemistry within the WRF model, Atmos. Environ., 39, 6957–6975, 2005.

Guenther, A., Karl, T., Harley, P., Wiedinmyer, C., Palmer, P. I., and Geron, C.: Estimates of global terrestrial isoprene emissions using MEGAN (Model of Emissions of Gases and Aerosols from Nature), Atmos. Chem. Phys., 6, 3181–3210, doi:10.5194/acp-6-3181-2006, 2006.

Gustafsson, O., Krusa, M., Zencak, Z., Sheesley, R. J., Granat, L., Engstrom, E., Praveen, P. S., Rao, P. S. P., Leck, C., and Rodhe, H.: Brown Clouds over South Asia: biomass or Fossil Fuel Combustion?, Science, 323, 495–498, 2009.

Hong, S.-Y., Noh, Y., and Dudhia, J.: A new vertical diffusion package with an explicit treatment of entrainment processes, Mon. Weather Rev., 134, 2318–2341, 2006.

Iacono, M. J., Delamere, J. S., Mlawer, E. J., Shephard, M. W., Clough, S. A., and Collins, W. D.: Radiative forcing by long–lived greenhouse gases: calculations with the AER radiative transfer models, J. Geophys. Res., 113, D13103, doi:10.1029/2008JD009944, 2008.

Knote, C., Hodzic, A., Jimenez, J. L., Volkamer, R., Orlando, J. J., Baidar, S., Brioude, J., Fast, J., Gentner, D. R., Goldstein, A. H., Hayes, P. L., Knighton, W. B., Oetjen, H., Setyan, A.,

ACPD
14, 30727–30759, 2014

Stark, H., Thalman, R., Tyndall, G., Washenfelder, R., Waxman, E., and Zhang, Q.: Simulation of semi-explicit mechanisms of SOA formation from glyoxal in aerosol in a 3-D model, Atmos. Chem. Phys., 14, 6213–6239, doi:10.5194/acp-14-6213-2014, 2014.

Kumar, R., Naja, M., Pfister, G. G., Barth, M. C., and Brasseur, G. P.: Simulations over South Asia using the Weather Research and Forecasting model with Chemistry (WRF-Chem): set-up and meteorological evaluation, Geosci. Model Dev., 5, 321–343, doi:10.5194/gmd-5-321-2012, 2012a.

Kumar, R., Naja, M., Pfister, G. G., Barth, M. C., Wiedinmyer, C., and Brasseur, G. P.: Simulations over South Asia using the Weather Research and Forecasting model with Chemistry (WRF-Chem): chemistry evaluation and initial results, Geosci. Model Dev., 5, 619–648, doi:10.5194/gmd-5-619-2012, 2012b.

Kumar, R., Naja, M., Pfister, G. G., Barth, M. C., and Brasseur, G. P.: Source attribution of carbon monoxide in India and surrounding regions during wintertime, J. Geophys. Res., 118, 1981–1995, doi:10.1002/jgrd.50134, 2013.

Kumar, R., Barth, M. C., Pfister, G. G., Naja, M., and Brasseur, G. P.: WRF-Chem simulations of a typical pre-monsoon dust storm in northern India: influences on aerosol optical properties and radiation budget, Atmos. Chem. Phys., 14, 2431–2446, doi:10.5194/acp-14-2431-2014, 2014a.

Kumar, R., Barth, M. C., Madronich, S., Naja, M., Carmichael, G. R., Pfister, G. G., Knote, C., Brasseur, G. P., Ojha, N., and Sarangi, T.: Effects of dust aerosols on tropospheric chemistry during a typical pre-monsoon season dust storm in northern India, Atmos. Chem. Phys., 14, 6813–6834, doi:10.5194/acp-14-6813-2014, 2014b.

Lau, K. M., Kim, M. K., and Kim, K. M.: Asian summer monsoon anomalies induced by aerosol direct forcing: the role of the Tibetan Plateau, Clim. Dynam., 26, 855–864, doi:10.1007/s00382-006-0114-z, 2006.

Lawrence, M. G. and Lelieveld, J.: Atmospheric pollutant outflow from southern Asia: a review, Atmos. Chem. Phys., 10, 11017–11096, doi:10.5194/acp-10-11017-2010, 2010.

Lu, Z. and Streets, D. G.: The Southeast Asia Composition, Cloud, Climate Coupling Regional Study Emission Inventory, available at: http://bio.cgrer.uiowa.edu/SEAC4RS/emission.html, last access: 24 August 2014, 2012.

Marrapu, P., Cheng, Y., Beig, G., Sahu, S., Srinivas, R., and Carmichael, G. R.: Air quality in Delhi during the Commonwealth Games, Atmos. Chem. Phys., 14, 10619–10630, doi:10.5194/acp-14-10619-2014, 2014.

ACPD
14, 30727–30759, 2014

Menon, S., Koch, D., Beig, G., Sahu, S., Fasullo, J., and Orlikowski, D.: Black carbon aerosols and the third polar ice cap, Atmos. Chem. Phys., 10, 4559–4571, doi:10.5194/acp-10-4559-2010, 2010.
Moorthy, K. K., Satheesh, S. K., and Babu, S. S.: Integrated Campaign for Aerosols, Gases and Radiation Budget (ICARB): an overview, J. Earth Syst. Sci., 117, 243–262, 2008.
Morrison, H., Thompson, G., and Tatarskii, V.: Impact of Cloud Microphysics on the Development of Trailing Stratiform Precipitation in a Simulated Squall Line: comparison of One– and Two–Moment Schemes, Mon. Weather Rev., 137, 991–1007, 2009.
Nair, V. S., Babu, S. S., and Moorthy, K. K.: Aerosol characteristics in the marine atmospheric boundary layer over the Bay of Bengal and Arabian Sea during ICARB: spatial distribution and latitudinal gradients, J. Geophys. Res., 113, D15208, doi:10.1029/2008JD009823, 2008.
Nair, V. S., Babu, S. S., Moorthy, K. K., Sharma, A. K., and Ajai, A. M.: Black carbon aerosols over the Himalayas: direct and surface albedo forcing, Tellus B, 65, 19738, doi:10.3402/tellusb.v65i0.19738, 2013.
Nair, V. S., Solmon, F., Giorgi, F., Mariotti, L., Babu, S. S., and Moorthy, K. K.: Simulation of South Asian aerosols for regional climate studies, J. Geophys. Res., 117, D04209, doi:10.1029/2011JD016711, 2012.
Neu, J. L. and Prather, M. J.: Toward a more physical representation of precipitation scavenging in global chemistry models: cloud overlap and ice physics and their impact on tropospheric ozone, Atmos. Chem. Phys., 12, 3289–3310, doi:10.5194/acp-12-3289-2012, 2012.
Pathak, B., Kalita, G., Bhuyan, K., Bhuyan, P. K., and Moorthy, K. K.: Aerosol temporal characteristics and its impact on shortwave radiative forcing at a location in the northeast of India, J. Geophys. Res., 115, D19204, doi:10.1029/2009jd013462, 2010.
Pfister, G. G., Avise, J., Wiedinmyer, C., Edwards, D. P., Emmons, L. K., Diskin, G. D., Podolske, J., and Wisthaler, A.: CO source contribution analysis for California during ARCTAS-CARB, Atmos. Chem. Phys., 11, 7515–7532, doi:10.5194/acp-11-7515-2011, 2011.
Pöschl, U.: Atmospheric aerosols: composition, transformation, climate and health effects, Angew. Chem. Int. Edit., 44, 7520–7540, 2005.
Ram, K., Sarin, M. M., and Tripathi, S. N.: A 1 year record of carbonaceous aerosols from an urban site in the Indo–Gangetic Plain: characterization, sources and temporal variability, J. Geophys. Res., 115, D24313, doi:10.1029/2010jd014188, 2010.

ACPD
14, 30727–30759, 2014

Ramanathan, V. and Carmichael, G.: Global and regional climate changes due to black carbon, Nat. Geosci., 1, 221–227, 2008.
Ramanathan, V., Chung, C., Kim, D., Bettge, T., Buja, L., Kiehl, J. T., Washington, W. M., Fu, Q., Sikka, D. R., and Wild, M.: Atmospheric Brown Clouds: impacts on South Asian Climate and Hydrological Cycle, P. Natl. Acad. Sci. USA, 102, 5326–5333, 2005.
Reddy, M. S., Boucher, O., Balkanski, Y., and Schulz, M.: Aerosol optical depths and direct radiative perturbations by species and source types, Geophys. Res. Lett., 32, L12803, doi:10.1029/2004GL021743, 2005.
Satheesh, S. K. and Ramanathan, V.: Large differences in tropical aerosol forcing at the top of the atmosphere and Earth's surface, Nature, 405, 60–62, 2000.
Skamarock, W. C., Klemp, J. B., Dudhia, J., Gill, D. O., Barker, D. M., Wang, W., and Powers, J. G.: A description of the advancedresearch WRF version 2, NCAR Tech. Note, NCAR/TN-468+STR, Natl. Cent. for Atmos. Res., Boulder, CO, available at: http://wrf-model.org/wrfadmin/publications.php, last access: 24 August 2014, 2008.
Srivastava, S., Lal, S., Venkataramani, S., Gupta, S., and Sheel, V.: Surface distributions of O_3, CO and hydrocarbons over the Bay of Bengal and the Arabian Sea during pre-monsoon season, Atmos. Environ., 47, 459–467, 2012.
Tewari, M., Chen, F., Wang, W., Dudhia, J., LeMone, M. A., Mitchell, K., Ek, M., Gayno, G., Wegiel, J., and Cuenca, R. H.: Implementation and verification of the unified NOAH land surface model in the WRF model, 20th Conference on Weather Analysis and Forecasting/16th Conference on Numerical Weather Prediction, Boulder, National Center for Atmospheric Research, June 22-25 2004, 11–15, 2004.
Tie, X., Madronich, S., Walters, S., Edwards, D. P., Ginoux, P., Mahowald, N., Zhang, R., Lou, C., and Brasseur, G.: Assessment of the global impact of aerosols on tropospheric oxidants, J. Geophys. Res., 110, D03204, doi:10.1029/2004JD005359, 2005.
Unger, N., Shindell, D. T., and Wang, S.: Climate forcing by the on-road transportation and power generation sectors, Atmos. Environ., 43, 3077–3085, doi:10.1016/j.atmosenv.2009.03.021, 2009.
Unger, N., Bond, T. C., Wang, J. S., Koch, D. M., Menon, S., Shindell, D. T., and Bauer, S.: Attribution of climate forcing to economic sectors, P. Natl. Acad. Sci. USA, 107, 3382–3387, doi:10.1073/pnas.0906548107, 2010.

ACPD
14, 30727–30759, 2014

Verma, S., Venkataraman, C., and Boucher, O.: Attribution of aerosol radiative forcing over India during the winter monsoon to emissions from source categories and geographical regions, Atmos. Environ., 45, 4398–4407, 2011.

Wesely, M. L.: Parameterization of surface resistance to gaseous dry deposition in regional-scale numerical models, Atmos. Environ., 23, 1293–1304, doi:10.1016/0004-6981(89)90153-4, 1989.

Wiedinmyer, C., Akagi, S. K., Yokelson, R. J., Emmons, L. K., Al-Saadi, J. A., Orlando, J. J., and Soja, A. J.: The Fire INventory from NCAR (FINN): a high resolution global model to estimate the emissions from open burning, Geosci. Model Dev., 4, 625–641, doi:10.5194/gmd-4-625-2011, 2011.

Yasunari, T. J., Bonasoni, P., Laj, P., Fujita, K., Vuillermoz, E., Marinoni, A., Cristofanelli, P., Duchi, R., Tartari, G., and Lau, K.-M.: Estimated impact of black carbon deposition during pre-monsoon season from Nepal Climate Observatory – Pyramid data and snow albedo changes over Himalayan glaciers, Atmos. Chem. Phys., 10, 6603–6615, doi:10.5194/acp-10-6603-2010, 2010.

Zaveri, R., Easter, R., Fast, J., and Peters, L.: Model for simulating aerosol interactions and chemistry (MOSAIC), J. Geophys. Res., 113, D13204, doi:10.1029/2007JD008782, 2008.

Zhang, X. Y., Wang, Y. Q., Zhang, X. C., Guo, W., and Gong, S. L.: Carbonaceous aerosol composition over various regions of China during 2006, J. Geophys. Res., 113, D14111, doi:10.1029/2007jd009525, 2008.

ACPD
14, 30727–30759, 2014

Table 1. WRF-Chem simulated BC mass concentration (mean ± SD) averaged over the period of 18 March to 11 May 2006, and observed range of average values during March–May at nine inland stations located in the model domain. The observed BC values are taken from the papers listed in the reference column.

Site Name	(Lat, Lon, Alt)	Mean Observed range (Mar–May)	WRF-Chem (18 Mar–11 May 2006)	References
Delhi	(28.6° N, 77.2° E, 260 m)	8–12 $\mu g\,m^{-3}$	6.0 ± 3.7 $\mu g\,m^{-3}$	Beegum et al. (2009)
Kanpur	(26.4° N, 80.3° E, 142 m)	2–5 $\mu g\,m^{-3}$	4.7 ± 2.7 $\mu g\,m^{-3}$	Ram et al. (2010)
Kharagpur	(22.5° N, 87.5° E, 28 m)	2–5 $\mu g\,m^{-3}$	7.4 ± 8.2 $\mu g\,m^{-3}$	Beegum et al. (2009)
Dibrugarh	(27.3° N, 94.6° E, 111 m)	5–10 $\mu g\,m^{-3}$	3.0 ± 2.1 $\mu g\,m^{-3}$	Pathak et al. (2010)
Trivandrum	(8.5° N, 76.9° E, 3 m)	1.8–3 $\mu g\,m^{-3}$	1.6 ± 0.9 $\mu g\,m^{-3}$	Beegum et al. (2009)
Minicoy	(8.3° N, 73.0° E, 1 m)	0.065–0.22 $\mu g\,m^{-3}$	0.32 ± 0.52 $\mu g\,m^{-3}$	Beegum et al. (2009)
Port-Blair	(11.6° N, 92.7° E, 60 m)	1.3–1.8 $\mu g\,m^{-3}$	0.8 ± 0.8 $\mu g\,m^{-3}$	Beegum et al. (2009)
Nainital	(29.4° N, 79.5° E, 1958 m)	0.8–1.5 $\mu g\,m^{-3}$	0.9 ± 0.5 $\mu g\,m^{-3}$	Beegum et al. (2009)
Nagarkot	(27.7° N, 85.5° E, 2150 m)	1.5 $\mu g\,m^{-3}$	1.1 ± 0.9 $\mu g\,m^{-3}$	Carrico et al. (2003)
Lhasa	(29.7° N, 91.1° E, 3663 m)	2–3 $\mu g\,m^{-3}$	0.5 ± 0.3 $\mu g\,m^{-3}$	Zhang et al. (2008)
Langtang	(28.1° N, 85.6° E, 3920 m)	0.5 $\mu g\,m^{-3}$	0.6 ± 0.4 $\mu g\,m^{-3}$	Carrico et al. (2003)
NCO-P	(28.0° N, 86.8° E, 5079 m)	0.2–0.4 $\mu g\,m^{-3}$	0.4 ± 0.3 $\mu g\,m^{-3}$	Bonasoni et al. (2010)

ACPD
14, 30727–30759, 2014

Table 2. Parameterization used for selected atmospheric processes in WRF-Chem.

Process	Parameterization
Cloud microphysics	Morrison double moment (Morrison et al., 2009)
Radiation	RRTMG short- and long-wave (Iacono et al., 2008)
Surface layer	MM5 similarity scheme (Beljaars, 1994)
Land surface model	Noah land surface (Tewari et al., 2004)
Planetary boundary layer	Yonsei university scheme (Hong et al., 2006)
Cumulus parameterization	Grell-3D (Grell and Devenyi, 2002)
Gas-phase chemistry	MOZART (Emmons et al., 2010; Knote et al., 2014)
Photolysis	Fast Troposphere Ultraviolet Visible (Tie et al., 2005)
Dry deposition	Wesely (Wesely, 1989)
Wet deposition	Neu and Prather (Neu and Prather, 2012)
Biogenic emissions	MEGAN (Guenther et al., 2006)
Dust emissions	GOCART (Ginoux et al., 2001)

ACPD
14, 30727–30759, 2014

Table 3. Near surface mass concentration ($ng\,m^{-3}$) of total anthropogenic BC (BC-ANT) and different anthropogenic regional BC tracers during the ICARB period along the ship-track in the AS and BoB, and over seven geogrpahical regions. Percentage contribution of each tracer to BC-ANT is also given in parenthesis. All numbers are rounded-off to the nearest whole number value. Numbers in bold font represent the contribution of local sources to the anthropogenic BC mass concentration of that region. BR and OT represent Burma and Other regions, respectively.

Region	BC-ANT[a]	BC-NI[a]	BC-WI[a]	BC-EI[a]	BC-SI[a]	BC-BR[a]	BC-OT[a]
Along the ICARB ship-track							
AS	241 ± 457	7 ± 6 (3 %)	22 ± 30 (9 %)	4 ± 4 (2 %)	199 ± 146 (83 %)	–	9 ± 10 (4 %)
BoB	1019 ± 1012	143 ± 139 (14 %)	82 ± 52 (8 %)	450 ± 748 (44 %)	329 ± 307 (32 %)	1 ± 1 (–)	14 ± 18 (1 %)
Geographical Regions							
North India	1082 ± 566	**985 ± 545 (91 %)**	19 ± 17 (2 %)	54 ± 51 (5 %)	9 ± 11 (1 %)	–	15 ± 3 (1 %)
West India	1483 ± 790	255 ± 192 (17 %)	**1044 ± 637 (70 %)**	78 ± 75 (5 %)	87 ± 68 (6 %)	– –	17 ± 5 (1 %)
East India	2842 ± 1049	232 ± 106 (8 %)	83 ± 34 (3 %)	**2246 ± 1029 (79 %)**	244 ± 114 (9 %)	24 ± 15 (1 %)	14 ± 5 (–)
South India	3390 ± 1021	71 ± 55 (2 %)	151 ± 69 (4 %)	89 ± 133 (3 %)	**3056 ± 941 (90 %)**	–	21 ± 7 (1 %)
Burma	1090 ± 271	129 ± 59 (12 %)	66 ± 28 (6 %)	418 ± 173 (38 %)	180 ± 6 (17 %)	**275 ± 120 (25 %)**	22 ± 19 (2 %)
AS	167 ± 101	11 ± 12 (7 %)	27 ± 29 (16 %)	3 ± 3 (2 %)	111 ± 74 (67 %)	–	15 ± 7 (9 %)
BoB	812 ± 774	110 ± 90 (14 %)	68 ± 32 (8 %)	384 ± 631 (47 %)	224 ± 112 (28 %)	11 ± 19 (1 %)	16 ± 6 (2 %)

[a] Mean±Sigma (SD).

ACPD
14, 30727–30759, 2014

Table 4. Average±SD in mass concentration ($ng\,m^{-3}$) of total BC, BC from anthropogenic sources (BC-ANT), from biomass burning (BC-BB), from model domain boundaries (BC-BDY), from residential (BC-RES), industrial (BC-IND), transportation (BC-TRA) and power generation (BC-POW) emissions averaged over South Asia (60–100° E, 5–37° N) during the ICARB period (18 March–11 May). The SD was calculated from all the BC values in South Asia and thus represents the spatial variability of modeled average BC values in South Asia.

Total BC	BC-ANT	BC-BB	BC-BDY	BC-RES	BC-IND	BC-TRA	BC-POW
1480 ± 5920	1030 ± 4770	415 ± 3420	35 ± 10	505 ± 880	390 ± 4490	130 ± 230	5 ± 65

ACPD
14, 30727–30759, 2014

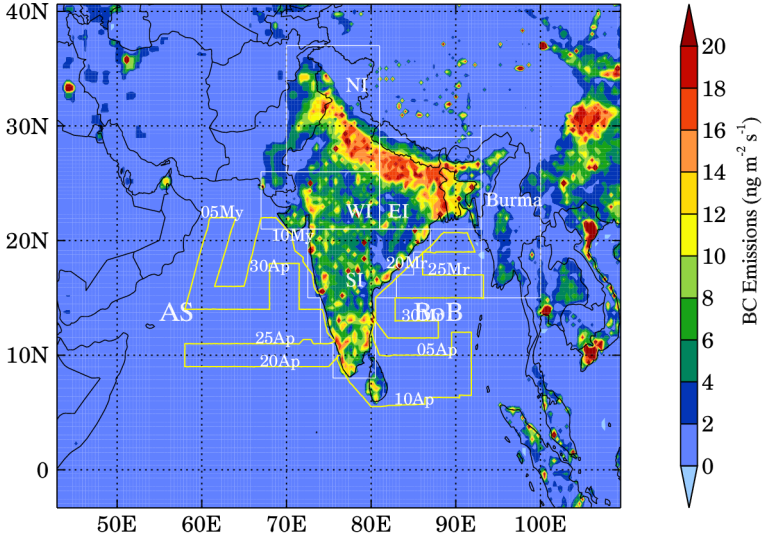

Figure 1. Spatial distribution of anthropogenic BC emissions over the model domain. Different regions from which BC emissions are tagged are shown with the Bay of Bengal and the Arabian Sea. Yellow line represents the ICARB ship-track, with the number standing for day of Month: Mr (March), Ap (April) and My (May). NI, WI, EI and SI represent North, West, East and South India, respectively.

ACPD
14, 30727–30759, 2014

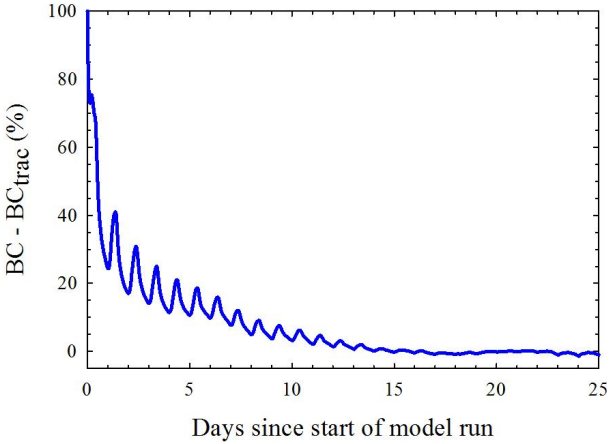

Figure 2. Time series of percentage difference between total simulated BC and sum of all the BC tracers (BC_{trac} = BC-ANT + BC-BB + BC-BDY).

ACPD
14, 30727–30759, 2014

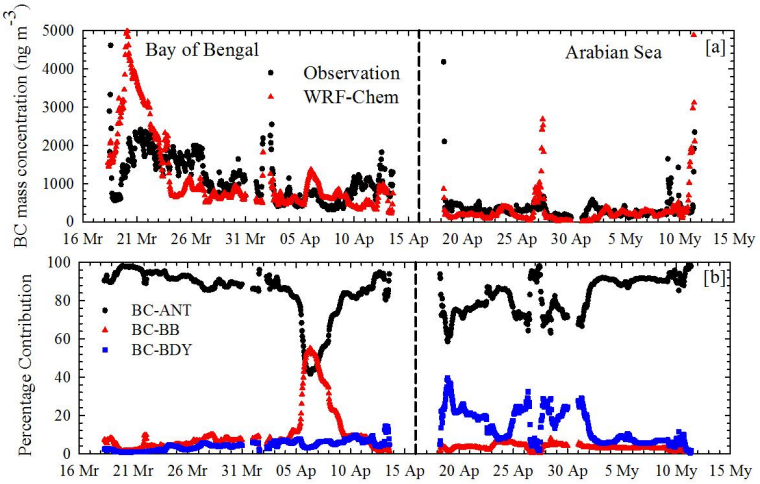

Figure 3. (a) WRF-Chem predicted and measured BC along the ICARB ship track during the ICARB period. **(b)** Percentage contributions of BC-ANT, BC-BB and BC-BDY to modeled BC.

ACPD
14, 30727–30759, 2014

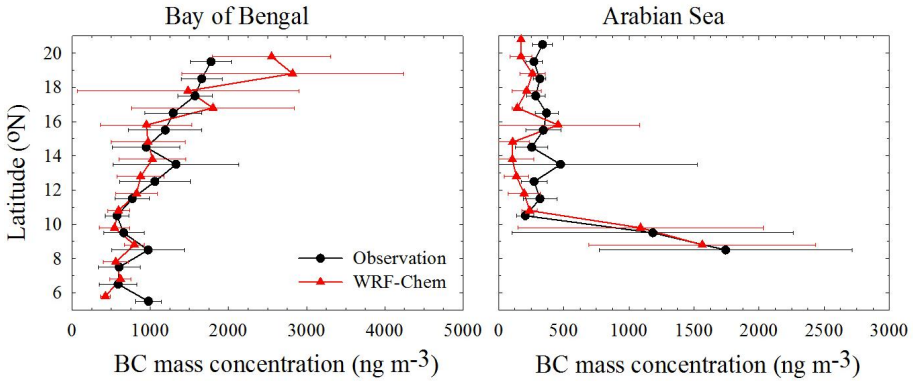

Figure 4. WRF-Chem predicted and observed latitudinal gradients in BC mass concentrations along the ICARB ship-track in the Bay of Bengal and Arabian Sea regions. Horizontal bars represents one sigma (SD) variation in BC mass concentration averaged over a 1° latitude bin.

ACPD
14, 30727–30759, 2014

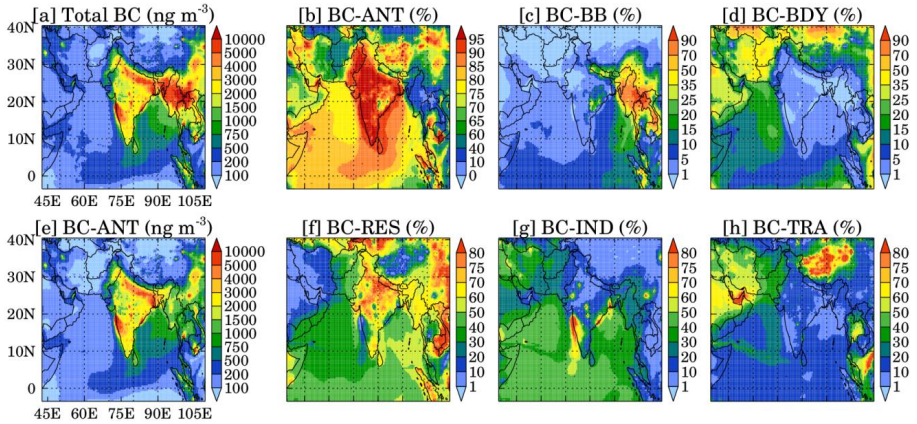

Figure 5. Spatial distributions of **(a)** total BC and **(e)** total anthropogenic BC mass concentration averaged over the ICARB period. Percentage contributions of BC-ANT **(b)**, BC-BB **(c)**, and BC-BDY **(d)** to total BC, and BC-RES **(f)**, BC-IND **(g)** and BC-TRA **(h)** to total anthropogenic BC.

ACPD
14, 30727–30759, 2014

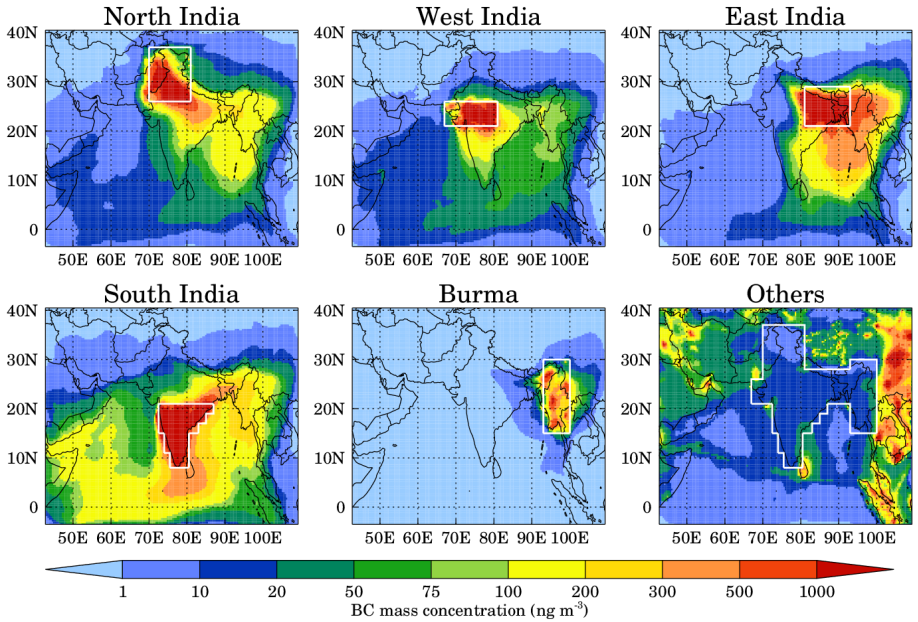

Figure 6. Spatial distributions of anthropogenic BC emitted from North, West, East and South India, Burma, and other regions during the ICARB period. White solid lines mark the geographical boundaries of different regions.

ACPD
14, 30727–30759, 2014